



Effect of Ferric Nanoparticles on Monoaminoxidase and Acetylcholinesterase in Healthy Human Sera

FADHEL M. HUSEEIN, SHAEMAA H. ABDULSADA*, WESSAL M. KHAMIS, SALMA ABDULREDHA and BAYADER F. ABBAS

Chemistry Department, College of Science, Al-Mustansiryah University, Baghdad, Iraq

*Corresponding author: Email: wessalmetaab@yahoo.com; wessalmetaab@uomustansiryah.edu.iq

Received: 13 February 2018;

Accepted: 28 March 2018;

Published online: 30 June 2018;

AJC-18967

In this study the Fe_2O_3 nanoparticles were prepared by sol-gel method. The size distributions of the metals nanoparticles were examined by FTIR spectrophotometer, atomic force microscopy and X-ray diffraction which illustrated that the nanoparticles were with hexagonal shape having averaged diameter of 54 nm derived from oleic acid. At the other side the nanoparticles prepared for carboxylic acid were irregular and unsystematic distributed with a maximum value of 0.38 and 2.9 nm exhibits morphology with a root-mean square (RMS) roughness of 0.077 and 0.494 nm for carboxylic acid. The effect of Fe_2O_3 nanoparticles were studied on the activities of monoaminoxidase (MAO) and acetylcholinesterase (AChE) in sera. Ferric nanoparticles demonstrated inhibitor effect on MAO and AChE and these effect increase with increasing the concentration of nanoparticles. The values of V_{\max} and K_m were achieved and calculated for these nanoparticales.

Keywords: Ferric Nanoparticales, Monoaminoxidase enzyme, Acetylcholinesterase enzyme.

INTRODUCTION

Hematite nanoparticles ($\alpha\text{-Fe}_2\text{O}_3$) have important properties in the fields of nanotechnology and nanoscience. These properties can be briefed by its superior characters in nano toxicity, chemical stability, low costs and durability [1]. The most utilized transition metal oxide of technological importance are the iron oxides with 16 known oxide and oxy-hydroxide (*i.e.*, five polymorphs of FeOOH , four of Fe_2O_3 (*i.e.*, hematite $\alpha\text{-Fe}_2\text{O}_3$, magnetite $\gamma\text{-Fe}_2\text{O}_3$ then $\beta\text{-Fe}_2\text{O}_3$ and $\epsilon\text{-Fe}_2\text{O}_3$ which are the less occurring ones [2,3]. The most popular and significant metal oxide is hematite ($\alpha\text{-Fe}_2\text{O}_3$) [4].

Hematite ($\alpha\text{-Fe}_2\text{O}_3$) can be made ready by various procedures such as sol-gel, micro emulsion, co-precipitations and solid state reaction [5]. Sol-gel method is the most popular one because it is low-cost and popular method to produce $\alpha\text{-Fe}_2\text{O}_3$ nanoparticles at a temperature (700 °C). In this paper the $\alpha\text{-Fe}_2\text{O}_3$ nanoparticles were provided from metal chloride and carboxylic acid as chelating agent by sol-gel process and the effect of these nanoparticles on MAO and AChE activity were studied kinetically.

The characteristics of the nanoparticles were studied by AFM, XRD, SEM and FTIR analysis. Jiao and his co-workers [6] prepared ordered mesoporous $\alpha\text{-Fe}_2\text{O}_3$ with crystalline walls through silica template, Li and his co-workers [7] have reported that $\alpha\text{-Fe}_2\text{O}_3$ synthesized by hydrothermal method. Zhang *et al.* [8] employed the sol-gel route to prepare hematite

nanoparticles starting from a 1:1 ratio of ferric nitrate and citric acid. Acetylcholinesterase (EC.3.1.1.7) is the hydrolase enzyme found in nervous tissues [9]. Acetylcholinesterase associated with nervous system disease such as Alzheimer disease and schizophrenia [10], AChE inhibitors used to reduce hydrolysis of acetyl choline and treatment of nervous diseases. Monoaminoxidase (EC. 1.4.3.4) is the enzyme that oxidize various amine in the body to produce H_2O_2 and aldehyde. There are two main type of the enzyme MAO-A and MAO-B [11].

Monoaminoxidase inhibitors have the ability to reduce production of peroxide, which increase neuronal damage and cause nervous system disease like Alzheimer and Parkinson disease. Monoaminoxidase inhibitor has been used in treatment of nervous disease [12].

EXPERIMENTAL

All chemicals were equipped by BDH and Fluka.

Preparation of $\alpha\text{-Fe}_2\text{O}_3$ using oleic acid by sol-gel method:

$\alpha\text{-Fe}_2\text{O}_3$ nanoparticles were prepared by sol-gel method using (1.62 g, 9.8 mmol) FeCl_3 was dissolved in 100 cm^3 distilled water with stirring for 30 min. Gelatin (oleic acid) (6.44 mL) was dissolved in a mount of absolute ethanol and 100 mL distilled water and then stirred for (30 min) and the mixture was heated at 60 °C for 1 h at pH 8 by adding drops of (30 %) ammonium hydroxide. As in the past, the obtained $\alpha\text{-Fe}_2\text{O}_3$ nanoparticles are red-brown colour.

Enzyme activity: Mix and centrifugation for 10 min then measure absorbance of supernatant at 242 nm.

This method use to indicate enzyme activity without nanoparticles, the same method has been used to study the effect of nanoparticles on MAO with replace 750 μL buffer with 500 μL buffer and 250 μL nanoparticles.

AChE assay: AChE activity was measured (manually) by using ELLMAN method [13] as follow:

50 mL of DTNB solution (0.001M) is added to 2.25 mL of sodium phosphate buffer (pH 7.3, 0.2 M), then 10 μL of serum was added, mixed well and (2 mL) of the mixture transferred to a measuring cell (3 mm), then 34 μL of acetylthiocholine iodide (ASCHI 0.06 M) is added, the change in absorbency is measured before and after adding the substrate at 430 nm.

This method was used to indicate enzyme activity without nanoparticles. The same method has been used to study the effect of nanoparticles on MAO with replace 2.25 mL buffer with 2 mL buffer and 0.25 mL nanoparticles.

TABLE-1 MAO ASSAY BY THE METHOD OF McEWEN AND COHEN [Ref. 13]		
Solutions	Test	Control
Serum	600 μL	600 μL
MAO buffer	750 μL	750 μL
Benzylamine	150 μL	–
Water bath shaking for 3 h at 37 °C		
Benzylamine	–	150 μL
Perchloric acid	150 μL	150 μL
Cyclohexane	1.5 mL	1.5 mL

Different concentrations of nanoparticles (0.01, 0.04, 0.06, 0.08 and 0.1) prepared from stock solution (1 mol/L). The inhibition percentage was calculated by using this equation:

$$\text{Inhibition (\%)} = 100 \left(\frac{\text{Activity in the presence of inhibitor}}{\text{Activity in the absence of inhibitor}} \right) \times 100$$

A constant concentration of inhibitor (0.1) M was used with different concentration of substrate to determine type of inhibition and by using line Weaver-Burk equation the following values were calculated: V_{map} , K_{map} and inhibition type.

RESULTS AND DISCUSSION

FTIR: The infrared spectroscopy FTIR is a surface sensitive technique which capable of providing information on the individual processes. Carboxylic acid can form complex compounds with metals by moral excellence of their carboxylic acid alcoholic (oxy) groups.

2-Oleic acid can form complex compound with metals by virtue of their carboxylic and alcoholic (oxy) groups. Fig. 1 shows the FTIR spectra of the $\alpha\text{-Fe}_2\text{O}_3$ synthesized by sol-gel method. It was observed that the bands from the C-O stretching vibrations of the free carboxyl groups are absent. The strong band at 536 and 569 cm^{-1} present in IR spectrum of calcined (700 °C) compound shows the presence of stretching and bending vibration of the intercalated M-O species. No peak at the presence of the two intense bands around 1647 and 1436

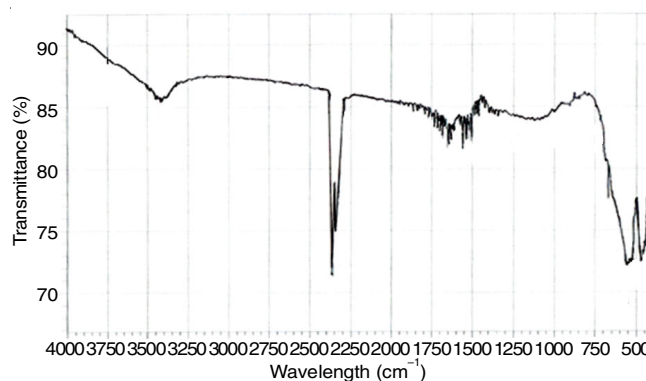


Fig. 1. FTIR spectra of $\alpha\text{-Fe}_2\text{O}_3$ prepared by sol-gel method using oleic acid after calcination at 700 °C

cm^{-1} indicating the complete replacement of H atoms on the carboxyl groups during the course of the process of complex formation between the carboxylic acid and the ferric ion [14]. The characteristic peak at 538 and 464 cm^{-1} for 2-oleic acid becomes very strong indicating the formation of stretching mode of $\alpha\text{-Fe}_2\text{O}_3$. This specifies the occurrence of hematite nanoparticles in calcined compounds.

Atomic force microscopy (AFM): The film structure and the surface morphology of the deposits materials have been studied by using atomic force microscopy (AFM). Fig. 2 shows the AFM images of surface morphology and the corresponding size distributions of the ferric oxide nanoparticles. It's clear from Fig. 2 that $\alpha\text{-Fe}_2\text{O}_3$ nanoparticles are hexagonal in shape having averaged diameter of 54 nm derived from oleic acid. The 3-dimensional (3D) AFM images of material nanoparticle in which the irregular and randomly distributed $\alpha\text{-Fe}_2\text{O}_3$ nanoparticles can be seen with a maximum value of 0.38 and 2.9 nm, respectively exhibits morphology with a root-mean square (RMS) roughness of 0.077 and 0.494 nm for carboxylic acid, respectively.

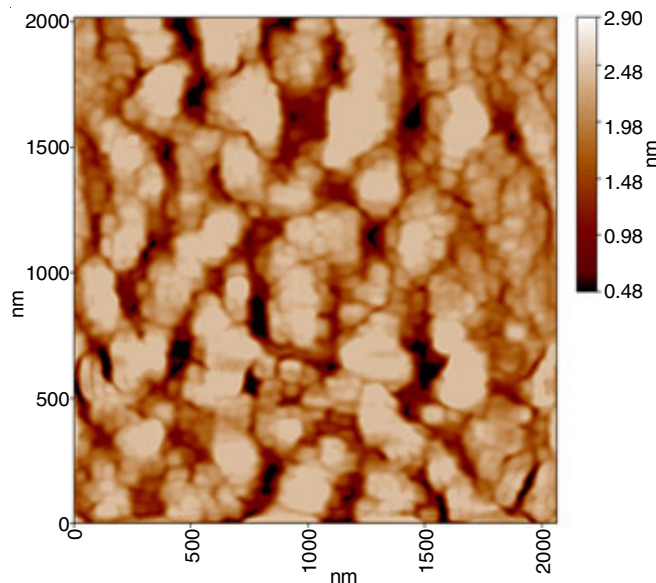


Fig. 2. AFM images for nanoparticles synthesized from oleic acid at 700 °C calcination through sol-gel

X-ray diffraction analysis: The X-ray diffraction patterns for hematite nanoparticles (calcined at 700 °C for 2 h) prepared

by sol-gel and photo methods using gelatin as a media was illustrated in Fig. 3. The complete transformation of $\gamma\text{-Fe}_2\text{O}_3$ to $\alpha\text{-Fe}_2\text{O}_3$ can be seen at 700 °C. These results are contradictory to those obtained by Karunakaran and Senthilvelan where they had reported the complete transformation at 880 °C [15]. The XRD peaks in whole angle range of 2θ from 10°-70° with Cu radiation (voltage 40 Kv and current 30 mA) $\lambda = 1.540 \text{ \AA}$ with speed 5°/min. It can be seen from Fig. 3 that 9 characteristic peaks were observed for $\alpha\text{-Fe}_2\text{O}_3$ nanoparticles ($2\theta = 24.2^\circ, 33.2^\circ, 35.6^\circ, 41.1^\circ, 49.5^\circ, 54.1^\circ, 57.4^\circ, 62.4^\circ$ and 64.0°). It was found that the ratio of the integrated intensities of (I/II) is higher than unity which correspond well to the standard XRD pattern of hematite. The diffraction peak of the synthesized $\alpha\text{-Fe}_2\text{O}_3$ are in good agreement with those reported in literatures [16]. Both the diffraction peaks and lattice parameters of the synthesized $\alpha\text{-Fe}_2\text{O}_3$ are in good agreement with reported in literatures [17-19].

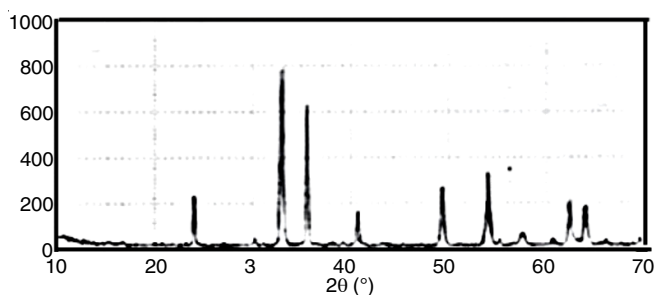


Fig. 3. XRD patterns of $\alpha\text{-Fe}_2\text{O}_3$ nanoparticles after calcined at 700 °C

Enzyme activity: This work was shown the effect of ferric nanoparticles on MAO and AChE.

Table-2 and Fig. 4 show the relation between AChE activity and nanoparticles concentration, when nanoparticles concentration increase from 0.01 M to 0.1 M, enzyme activity decrease from 6.46 to 1.61 mol/min/mL.

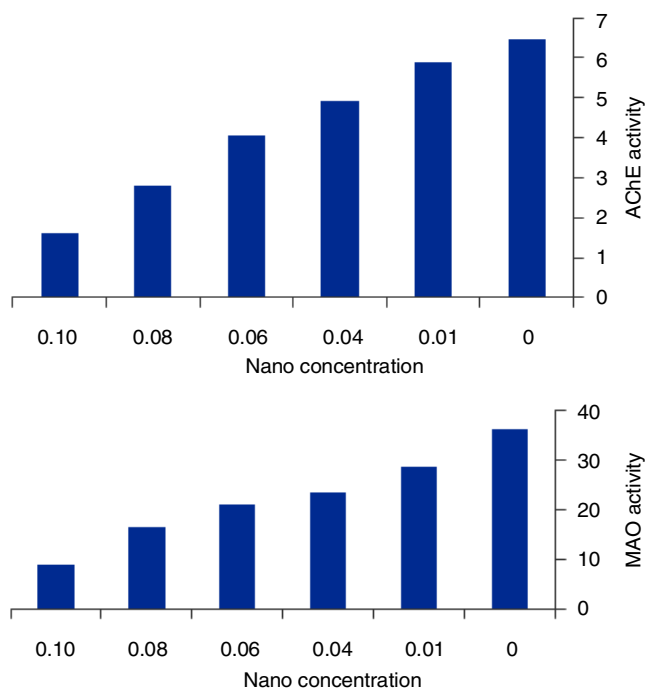


Fig. 4. Effect of different concentration of nanoparticles on AChE and MAO

Nano conc.	AChE activity ($\mu\text{mol}/3 \text{ min/mL}$)	Inhibition (%)
Nil	6.46	–
0.01	5.89	11.29
0.04	4.91	26.05
0.06	4.05	39.00
0.08	2.80	57.83
0.1	1.61	75.75

The relation between MAO activity and ferric nanoparticles concentration were shown at Table-3 and Fig. 4 which indicated the concentration of inhibitor increase from 36.11 to 8.94.

Nano conc.	MAO activity ($\mu\text{mol}/3 \text{ min/mL}$)	Inhibition (%)
Nil	36.11	–
0.01	28.64	20.68
0.04	23.43	35.40
0.06	21.02	41.79
0.08	16.33	54.78
0.1	8.94	75.24

At the same time the values which were pointed out at Table-4 and Fig. 5 were shown type of inhibition (uncompetitive with MAO and AChE) by using Lineweaver-Burk equation, V_m 62.5 with MAO and 0.05 with AChE, K_m 0.11, 0.04 with MAO and AChE, respectively.

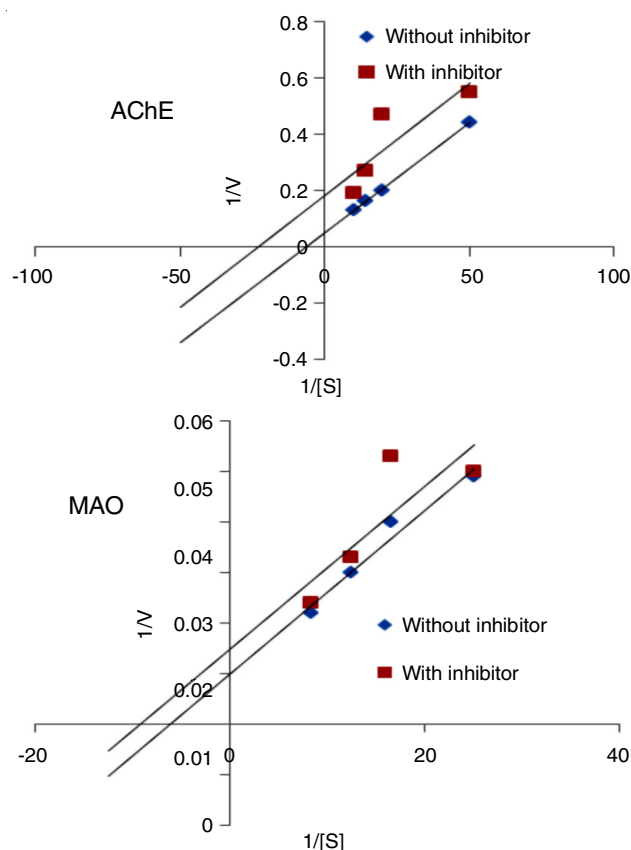


Fig. 5. Lineweaver burk equation of MAO and AChE

TABLE-4
KINETIC PARAMETERS OF MAO AND
AChE WITH Fe₂O₃ NANOPARTICLES

Enzymes	V _{max} (μmol/mL/min)	K _{map} [M]	Inhibition type
MAO	62.5	0.11	Un-competitive
AChE	0.05	0.04	Un-competitive

Some researches indicate that iron oxide nanoparticles have been used in treatment of cancer [20]. Other researches show the effect of other nanoparticles like gold and silver on MAO and AChE [21]. Ferric nanoparticles inhibit MAO and AChE because they may interact with functional group in active site of enzymes and cause protein denaturation.

REFERENCES

- M.F.R. Fouda, M.B. El-Kholy, S.A. Mostafa, A.I. Hussien, M.A. Wahba and M.F. El-Shahat, *Adv. Mater. Lett.*, **4**, 347 (2013); <https://doi.org/10.5185/amlett.2012.9421>.
- A. Ibrahim and B.A. Abubakar, *African J. Pure Appl. Chem.*, **7**, 114 (2013); <https://doi.org/10.5897/AJPAC12.002>.
- S. Bagheri, K.G. Chandrappa and S.B. Abd Hamid, *Res. J. Chem. Sci.*, **3**, 62 (2013).
- B. Lv, Y. Xu, D. Wu and Y. Sun, *J. Mater. Sci. Technol.*, **25**, 155 (2009).
- L. Zhang and Y. Wu, *J. Nanomater.*, **Article ID 640940** (2013); <https://doi.org/10.1155/2013/640940>.
- F. Jiao, A. Harrison, J.-C. Jumas, A.V. Chadwick, W. Kockelmann and P.G. Bruce, *J. Am. Chem. Soc.*, **128**, 5468 (2006); <https://doi.org/10.1021/ja0584774>.
- G.S. Li, R.L. Smith Jr., H. Inomata and K. Arai, *Mater. Res. Bull.*, **37**, 949 (2002); [https://doi.org/10.1016/S0025-5408\(02\)00695-5](https://doi.org/10.1016/S0025-5408(02)00695-5).
- J. Zhang, L.X. Rong, Y. Liu and B.Z. Dong, *Mater. Sci. Eng. A*, **351**, 224 (2003); [https://doi.org/10.1016/S0921-5093\(02\)00861-4](https://doi.org/10.1016/S0921-5093(02)00861-4).
- R. Wang and X.C. Tang, *Neurosignals*, **14**, 71 (2005); <https://doi.org/10.1159/000085387>.
- L. Davis, J.J. Britten and M. Morgan, *Anaesthesia*, **52**, 244 (1997); <https://doi.org/10.1111/j.1365-2044.1997.084-az0080.x>.
- C.W. Abell and S.W. Kwan, *Prog. Nucl. Acid Res. Mol. Biol.*, **65**, 129 (2001); [https://doi.org/10.1016/S0079-6603\(00\)65004-3](https://doi.org/10.1016/S0079-6603(00)65004-3).
- B. Mondovi and A.F. Agro, *Structure and Function of Amine Oxidases*, CRC Press, Boca Raton, FL (1982).
- C.M. Mcewen Jr. and J.D. Cohen, *J. Lab. Clin. Med.*, **62**, 766 (1963).
- G.L. Ellman, K.D. Courtney, V. Andres Jr. and R.M. Featherstone, *Biochem. Pharmacol.*, **7**, 88 (1961); [https://doi.org/10.1016/0006-2952\(61\)90145-9](https://doi.org/10.1016/0006-2952(61)90145-9).
- F. Bossa, E. Chiancone, A. Finazzi-Agrò and R. Strom, *Structure and Function Relationships in Biochemical Systems*, In: *Advances in Experimental Medicine and Biology*, Springer, Boston, USA, edn 1, vol 148 (1982).
- Ch. Karunakaran and S. Senthilvelan, *Catal. Commun.*, **6**, 159 (2005); <https://doi.org/10.1016/j.catcom.2004.11.014>.
- S. Karthikeyeni, T. Siva Vijayakumar, S. Vasanth, A. Ganesh, M. Manimegalai and P. Subramanian, *J. Acad. Ind. Res.*, **1**, 645 (2013).
- V.A. Sadykov, L.A. Isupova, S.V. Tsybulya, S.V. Cherepanova, G.S. Litvak, E.B. Burgina, G.N. Kustova, V.N. Kolomiichuk, V.P. Ivanov, E.A. Paukshtis, A.V. Golovin and E.G. Avvakumov, *J. Solid State Chem.*, **123**, 191 (1996); <https://doi.org/10.1006/jssc.1996.0168>.
- D.K. Bora, Ph.D. Thesis, Hematite and its Hybrid Nanostructures for Photoelectrochemical Water Splitting: How Do Properties Affect Functionality? Faculty of Science, University of Basel, Basel, Switzerland (2012).
- W.M. Shwe, M.M. Oo and S.S. Hlaing, *Int. J. Chem. Environ. Biol. Sci.*, **1**, 412 (2013).
- R. Thapa, J. Gorski, A. Bogedin, M. Maywood, C. Clement, S.H. Nasr, D. Hanna, X. Huang, B.J. Roth, G. Madlambayan and G.D. Wilson, *Int. J. Cancer Therapy Oncol.*, **4**, 1 (2016); <https://doi.org/10.14319/ijcto.42.4>.
- M.F. Farhat, M.A. Makhoulouf, A.M. El-Saghier, A. B.A. Mezoughi, S.M. Awhida and A.A.M. El-Mehdi, *Arabian J. Chem.*, **4**, 307 (2011); <https://doi.org/10.1016/j.arabjc.2010.06.051>.